Microscopic nature and optical properties of metastable defects in electron-irradiated GaAs

S. Kuisma, K. Saarinen, P. Hautojärvi, and C. Corbel*
Laboratory of Physics, Helsinki University of Technology, 02150 Espoo, Finland
(Received 23 October 1996)

Systematic correlation of infrared absorption and positron annihilation experiments allows us to identify two metastable defects in electron-irradiated GaAs. The first one is present already in as-grown material, and can be identified as the native $EL2$ defect by its photoquenching and subsequent thermal-annealing properties. The second one is introduced by irradiation at 300 K, and it disappears in thermal annealing at 520 K. Its metastable state is optically active, anneals at 70 K, and exhibits optical recovery at 25 K. Positron experiments indicate that both of these defects have a vacancy in their metastable state in good agreement with the vacancy-interstitial model of the As antisite defect. Therefore, the native defect is here attributed to an As antisite and the irradiation-induced one to an As antisite complex. The metastable state of the As_{Ga} complex can be generated with 1.075-eV photons and recovered with 1.35-eV photons with optical cross sections of 2×10^{-20} and 5×10^{-19} cm^2, respectively. The metastable state of the As_{Ga} complex absorbs 0.7−1.2-eV photons, indicating that it has ionization levels in the band gap. [S0163-1829(97)06815-X]

I. INTRODUCTION

The most fascinating property of the native $EL2$ defect in GaAs is its metastability. The defect can be converted to a metastable state by illumination with 1.1 eV $<h\nu<$1.3 eV light at low temperatures. The metastable state is electrically and optically inactive: its ionization levels are not in the band gap, and therefore it does not absorb infrared (IR) light. After illumination at $T<100$ K, the $EL2$ defect remains persistently in the metastable state until a thermal annealing at $T>120$ K is performed. The metastability of the $EL2$ defect can be theoretically explained by the vacancy-interstitial model[1] for an isolated As antisite defect. In the stable state the As antisite is on a substitutional lattice site, but in the metastable state it has relaxed along the [111] direction, leaving behind a Ga vacancy: $As_{Ga}\rightarrow V_{Ga}$-$As_i$. An internal optical transition can convert the defect from the stable to the metastable state, but these two states are separated by an energy barrier of about 0.3 eV, corresponding to an annealing temperature of 120 K.

Introduction of As antisite defects in electron irradiation of GaAs has been reported in several papers.[2–15] However, most infrared absorption studies have revealed only minor metastable effects, which have often been related to the native $EL2$ defect remaining in the sample after irradiation.[3,6,7] The detection of irradiation-induced $EL2$-like metastable defects has been reported in some electron-paramagnetic-resonance (EPR) and magnetic-circular-dichroism of absorption (MCDA) experiments.[4] Recently, MCDA measurements have revealed three different As antisite related defects with slightly different metastable properties.[16] However, no structural information on the metastable states of the irradiation-induced defects has been obtained in these experiments.

In good agreement with the vacancy-interstitial model, positron annihilation measurements in as-grown GaAs have manifested that the metastable state of the native $EL2$ defect contains a vacancy.[17] Experiments in electron-irradiated GaAs have shown that defects with a vacancy in the metastable state are also introduced by irradiation.[18] This metastable vacancy is similar to that related to the native $EL2$ defect, and therefore it has been associated with the atomic structure of the metastable state of the irradiation-induced As antisite defect.[18] However, some properties of the irradiation-induced defects are different from those of the native $EL2$ defect. In particular, the metastable state of the irradiation-induced defect is optically active, suggesting that it has ionization levels in the band gap.[19] The metastable effects in irradiated GaAs can also be optically recovered at 25 K, although this is not possible for the native $EL2$ defect. These differences can be explained by the presence of other defects which form complexes with the As antisite in irradiated GaAs.[18,19]

In this work, the systematic combination of positron annihilation and infrared absorption spectroscopies is used to study the optical properties and atomic structure of metastable defects in irradiated GaAs. Experiments in several samples irradiated to various electron fluences allow us to separate native defects from those introduced by irradiation. Further, the different metastable defects in GaAs can be distinguished by studying their photoquenching and subsequent thermal and optical recovery properties. In contrast to our earlier work,[19] the metastable changes in IR absorption are studied here at a wide photon energy range (0.7 eV $<h\nu<$1.4 eV), and the positron annihilation data are analyzed with the positron trapping model. This allows a quantitative correlation of the infrared absorption and positron annihilation results in terms of optical cross sections. Furthermore, we have investigated also the thermal stability of the metastable defects in irradiated GaAs.

The results show that there are two different metastable defects in electron-irradiated GaAs after annealing at 300 K. The first one is a native defect, and its concentration is not increased by irradiation. Its optically inactive metastable state anneals thermally at 120 K but cannot be optically recovered at 25 K. We conclude that this defect is the native $EL2$. The second metastable defect is introduced by irradiation and is not present in as-grown GaAs. Its metastable state absorbs IR light, anneals at 70 K, and exhibits optical recovery already at 25 K. Positron experiments show that both

defects have a similar vacancy in the metastable state, in good agreement with the vacancy-interstitial model for the As antisite defect. We thus attribute the native defect to an As antisite and the irradiation-induced defect to an As antisite complex. The As_{Ga} complex is most probably the arsenic-antisite–gallium-antisite antistructure pair detected earlier in MCDA experiments.[16] The metastable state of the irradiation-induced As_{Ga} complex can be generated by 1.075-eV illumination with a cross section of 2×10^{-20} cm^2, and it can be optically recovered by 1.35-eV light with a cross section of 5×10^{-19} cm^2. Unlike the native $EL2$ defect, the metastable state of the As_{Ga} complex absorbs light at $h\nu=0.7-1.2$ eV in a photoionization process. This indicates that the complex has ionization levels in the band gap in the metastable state. The irradiation-induced As_{Ga} complex recovers thermally at 520 K, whereas the native $EL2$ defect remains unchanged over this annealing stage.

The next section describes briefly the experimental methods used in this work. The infrared absorption results are presented in Sec. III, and they are correlated quantitatively to positron annihilation data in Sec. IV. The microscopic nature of the observed defects is discussed in Sec. V. Section VI treats the thermal stability of the irradiation-induced metastable defect, and Sec. VII concludes this work.

II. EXPERIMENTAL DETAILS AND ANALYSIS METHODS

A. Infrared absorption

Defects having energy levels in the energy gap are able to absorb light at lower energies than the band gap. The absorption coefficient α at a certain photon energy $h\nu$ is the superposition of various defects at concentrations $[d_i]$,

$$\alpha(h\nu)=\sum_i \sigma_i(h\nu)[d_i], \tag{1}$$

where σ_i is the effective cross section containing all the absorption processes related to the defect d_i.

The infrared absorption measurements of this work were performed at 30 K in an optical cryostat. Light from a 250-W halogen lamp was led to a monochromator and then to the sample with an optical fiber bundle. The photon energy range used for the illumination was $h\nu=0.7-1.5$ eV and the maximum photon flux $\phi=10^{16}$ cm^{-2} s^{-1}. The sample temperature could be varied from 30 to 300 K using a closed-cycle He cryocooler.

The incident intensity I_0 of the IR light was detected with a Si-Ge photodetector from a reference branch of the fiber bundle, and the intensity I transmitted through the sample was observed simultaneously with a Ge photodetector. The intensities were measured by collecting data every 10 s: every data point was measured by averaging 400 samples recorded with a sampling frequency of about 100 Hz. Within the experimental accuracy, the absorption was constant over the time needed to collect the 400 samples. In some cases the number of samples was reduced in order to ensure that the absorption was not altered during the collection. This collecting procedure limits the time scale for studied processes to larger than 10 s; on the other hand, the large number of data samples enables the observation of small changes in the absorption coefficient. The measured absorption values correspond to a steady-state situation caused by the probing illumination.

To compare absorption results in different samples and in different situations, the absorption coefficient was calculated from

$$I=I_0\exp(-\alpha x), \tag{2}$$

where x is the thickness of the sample. Due to experimental limitations, changes in α were precisely measured but the absolute values are accurate only within $\pm$ 0.5 cm^{-1}.

Mounting of the sample required reinstallation of the optical fiber stands, and, due to small differences in the illumination geometry, a difference of about 20% in the illumination intensity is possible from one sample to another. The photon flux and fluence values stated below are nominal.

B. Positron lifetime spectroscopy

Positron lifetime measurements were performed in a conventional way:[20] the positron and a 1.275-MeV γ are emitted simultaneously in a β^+ decay from the ^{22}Na isotope, and a fast-fast lifetime spectrometer was used to measure the time difference between the 1.275-MeV γ and the annihilation γ. Two identical sample pieces were sandwiched with a 30-μCi positron source, which consisted of carrier-free ^{22}NaCl deposited on a 1.5-μm-thick Al foil. The sample sandwich was mounted in the same optical cryostat that was used in the IR absorption measurements. Illuminations were also performed with the same setup. Further experimental details can be found in Ref. 21.

After subtracting the constant background and annihilations in the source material, the measured positron lifetime spectrum was analyzed with one or two exponential components

$$n(t)=n_0[I_1\exp(-t/\tau_1)+I_2\exp(-t/\tau_2)] \tag{3}$$

convoluted with the Gaussian resolution function of the spectrometer. Here n_0 is the total number of annihilation events, and I_i is the intensity of the decay mode with a positron lifetime τ_i. The average positron lifetime is defined by

$$\tau_{av}=I_1\tau_1+I_2\tau_2. \tag{4}$$

The average lifetime is insensitive to the decomposition procedure and coincides with the center of mass of the lifetime spectrum.

Positron lifetime spectroscopy yields microscopic information on vacancy defects in material. In a perfect semiconductor crystal positrons are delocalized in the lattice and annihilate with a free positron lifetime τ_b. Neutral and negative vacancies can trap positrons to localized states.[22] In these vacancies the electron density is lower than in the bulk, and thus positrons annihilate with a lifetime τ_v, which is longer than τ_b.

Positrons can also get trapped at Rydberg states around negative ions: this enables the detection of negative-ion-type defects in semiconductor materials. The negative ions are shallow traps for positrons, since the binding energy for positrons is less than 0.1 eV. At higher temperatures positrons start to escape thermally from the Rydberg states;[23] e.g., in

GaAs the thermal escape begins at 100 K.[24] Positrons trapped at negative ions annihilate with the same lifetime as free positrons.[24]

The concentration of defects trapping positrons can be estimated from the positron trapping rate κ, which is proportional to the defect concentration c_d:

$$\kappa = c_d \mu / N. \tag{5}$$

Here μ is the defect-specific trapping coefficient and N is the atomic density of the material. For neutral vacancies the trapping coefficient μ_v is temperature independent, and its value is typically $10^{15}\ \mathrm{s}^{-1}$.[25] For negative vacancies μ_v is roughly $2\times10^{15}\ \mathrm{s}^{-1}$ at 300 K,[26] and it increases by an order of magnitude when temperature decreases to 20 K.[22,27,28]

In practice, positron trapping at vacancies can be detected by measuring the average positron lifetime τ_{av}. Increase in τ_{av} above τ_b is a clear indication of vacancy defects in the sample. According to the trapping model,[29] the average positron lifetime is a superposition of the free positron lifetime τ_b, lifetimes τ_{vi} at vacancy defects i, and lifetime at the Rydberg states around negative ions $\tau_{st}=\tau_b$,

$$\tau_{\mathrm{av}} = \eta_b \tau_b + \sum_{i=1}^{l} \eta_{vi}\tau_{vi} + \eta_{st}\tau_b, \tag{6}$$

where η_b, η_{vi}, and η_{st} are the fractions of positrons annihilating at the defect-free bulk, vacancies, and shallow traps. The trapping fractions can be expressed in terms of positron trapping rates, which can be calculated from the measured average positron lifetime. If there are both vacancies and negative ions present in the sample, positron trapping rates at both these defects can be determined by measuring the average lifetime as a function of temperature.[18,26]

C. Samples

In this work two sets of electron-irradiated GaAs samples were studied. The first set consisted of four pairs of samples that were all cut from the same wafer of undoped semi-insulating GaAs. Three sample pairs were irradiated with 1.5-MeV electrons at 20 K with electron fluences of 1, 5, and $13\times10^{17}\ \mathrm{cm}^{-2}$, whereas a reference sample pair was left unirradiated. The samples with the largest irradiation fluence were annealed at 425 K, while the others were aged at room temperature.

The other set consisted of two pairs of undoped semi-insulating GaAs samples, both irradiated with 2-MeV electrons to an electron fluence of $5\times10^{17}\ \mathrm{cm}^{-2}$ at 300 K. After irradiation one pair was aged at room temperature, and the other was annealed at 520 K.

III. METASTABILITY OF THE ABSORPTION SPECTRUM IN ELECTRON-IRRADIATED GaAs

A. Photon-energy dependence of the absorption

The IR absorption of electron-irradiated GaAs as a function of the photon energy was measured before any illuminations at 25 K. Before the absorption measurement the sample was annealed in darkness at 200 K in order to recover all metastable effects, and it was checked that the photon flux used for the measurement did not affect absorption during the measurement time. The values obtained in this measurement are referred to as initial absorption in this paper.

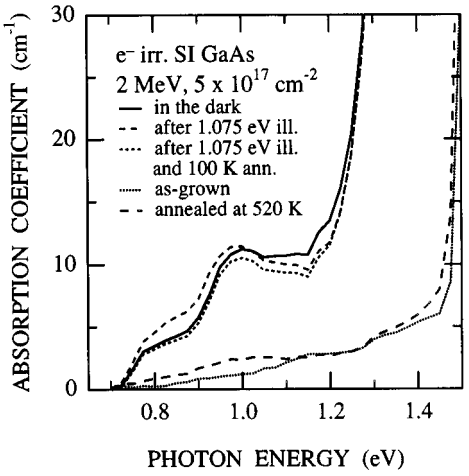

FIG. 1. Infrared absorption in electron-irradiated GaAs aged at 300 K as a function of photon energy. Measurement temperature was 25 K. Absorption before any illumination is marked with a solid line, after 1.075-eV illumination with a dashed line, and after a subsequent annealing at 100 K with a dotted line. Absorption in as-grown GaAs and in electron-irradiated GaAs annealed at 520 K are shown as well.

In electron-irradiated GaAs the absorption at photon energies $h\nu=0.7-1.4$ eV is clearly larger than in as-grown material. Figure 1 shows the results for GaAs irradiated with a 5×10^{17}-cm^{-2} fluence of 2-MeV electrons. The well-known features of absorption in electron-irradiated GaAs can be observed: a shoulder at 0.8 eV and a peak at 1.0 eV,[3,7] as well as a strong increase in absorption at photon energies just below band gap. Absorption related to the native $EL2$ defect, which dominates the IR absorption spectrum in as-grown GaAs,[30] is shown as reference in Fig. 1. In electron-irradiated GaAs absorption related to $EL2$ is largely masked by the absorption of the irradiation-induced defects.

B. Behavior of absorption during photoquenching

To study the photoquenching effects in IR absorption in electron-irradiated GaAs, the samples were illuminated at 25 K with various photon energies at $0.9\ \mathrm{eV}<h\nu<1.4$ eV and a constant photon flux of $10^{16}\ \mathrm{cm}^{-2}\ \mathrm{s}^{-1}$. Absorption was monitored simultaneously with the same photon energy as used for the photoquenching. Before the illuminations the sample was annealed in darkness at 200 K to remove all metastable effects.

The absorption coefficient as a function of the photoquenching time, $\alpha(t)$, behaves similarly in all the irradiated GaAs samples aged at room temperature. Results for the GaAs sample irradiated with 1.5-MeV electrons to a fluence of $5\times10^{17}\ \mathrm{cm}^{-2}$ are presented in Fig. 2. When illumination is turned on, $\alpha(t)$ starts to decrease with a time constant that depends on the photon energy (Fig. 2). For $h\nu=1.05$ eV this decrease lasts about 1000 s and for $h\nu=1.25$ eV about 5000 s. The decrease in absorption is observed with $0.9\ \mathrm{eV}<h\nu<1.4$ eV, and the magnitude of this decrease depends on the photon energy.

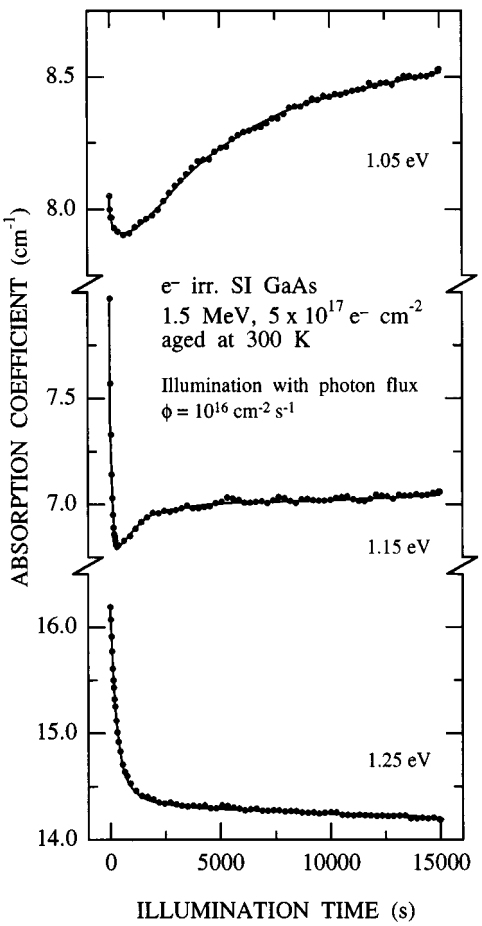

FIG. 2. Infrared absorption in electron-irradiated GaAs as a function of illumination time. The photon energies used for the illuminations are marked in the figure. Measurement temperature was 25 K, and absorption was measured with the same photon energy as the illumination occurred.

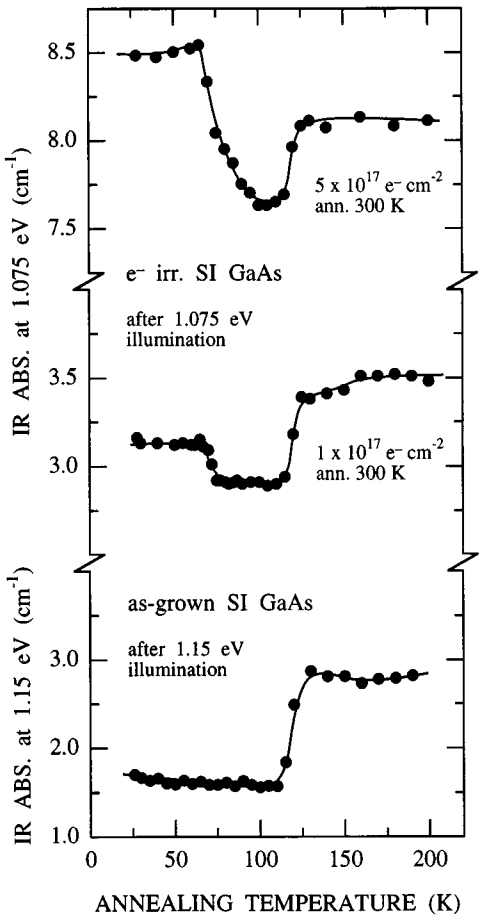

FIG. 3. Absorption coefficient at 1.075 eV as a function of annealing temperature in electron-irradiated GaAs. Measurement temperature was 25 K, and the sample was illuminated with 1.075-eV photons before the isochronal annealing. Illumination was performed and absorption was monitored with 1.15-eV photons in as-grown GaAs.

When the photoquenching is performed with 0.95−1.2-eV photons, the absorption coefficient goes through a minimum and then starts to increase with a much longer time constant. For example, the increase in absorption saturates after an illumination time of $t \approx 15\,000$ s when the sample is illuminated with 1.05-eV photons. The magnitude and the time constant of the increase depend on the photon energy. At $0.95\ \text{eV} < h\nu < 1.075\ \text{eV}$ the final absorption after a long illumination even exceeds the initial value observed before any photoquenching.

Both the decrease and increase in the absorption are persistent: when the illumination is turned off and the sample is kept in darkness at 25 K, the absorption coefficient has the same value when monitored after a long period of time. Only heating of the sample at temperatures $T > 120$ K recovers the initial value of absorption. Thus there are metastable changes, both an increase and a decrease, in the IR absorption in electron-irradiated GaAs.

C. Annealing behavior of the metastable changes in the absorption

The isochronal annealing behavior of the persistent changes in the IR absorption were studied after 1.075-eV and 1.15-eV illuminations. After an illumination lasting for 20 000 s with a photon flux of $10^{16}\ \text{cm}^{-2}\ \text{s}^{-1}$ at 25 K, the sample was kept at each annealing temperature for 10 min and then cooled back to 25 K for the absorption measurement. The absorption was monitored with the same photon energy as used for the illumination.

The annealing behavior of absorption is shown in Fig. 3 for the as-grown and 1.5-MeV electron-irradiated GaAs samples. After annealing at 60−80 K the absorption decreases in the irradiated but not in the as-grown samples. From this low level the absorption increases to the initial value after annealing at 120 K. The magnitude of this increase is the same in as-grown and electron-irradiated samples. In the irradiated material absorption at 1.15 and 1.075 eV behaves similarly: both annealing steps at 70 K and at 120 K are observed. In as-grown GaAs no annealing stage at 70 K is observed, and at 120 K absorption increases to the initial value before any illumination.

The magnitudes of the annealing steps at 70 and 120 K are plotted in Fig. 4 as functions of the electron-irradiation fluence. The changes are more clearly seen at a photon energy of 1.15 eV for the annealing step at 120 K and at 1.075 eV for the 60-K annealing stage. As seen in Fig. 4, the de-

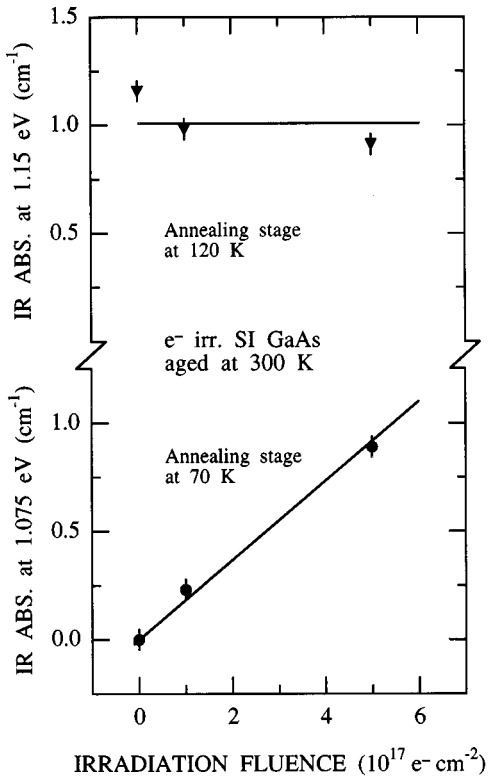

FIG. 4. Change in infrared absorption in isochronal annealing at 70 and 120 K compared to the absorption after 100-K annealing in electron-irradiated GaAs. Before the measurement the sample was illuminated with 1.075-eV photons (lower panel) or 1.15-eV photons (upper panel), and absorption was measured at 25 K at the same photon energy.

crease in absorption after 70-K annealing depends linearly on the irradiation fluence, and the annealing step at 120 K, on the other hand, is independent of the electron fluence.

D. Absorption related to the native and irradiation-induced metastable defects

The behavior of the absorption coefficient under illumination, an increase and a decrease with different time constants, and the two distinct annealing steps in the absorption suggest the presence of two different metastable defects in electron-irradiated GaAs. The decrease in the absorption and the annealing step at 120 K are related to one, and the increased absorption and annealing stage at 70 K to the other.

The two persistent transients in the absorption coefficient (Fig. 2) can be modeled with exponential decay terms and a constant background a

$$\alpha(t)=a+b\exp(-t/\tau_1)+c\exp(-t/\tau_2), \tag{7}$$

where τ_1 and τ_2 are the time constants, and b and c stand for the magnitude of the decrease ($b>0$) or increase ($c<0$) in absorption. The time constants, which depend on the illumination intensity, can be converted to optical cross sections σ: $\tau^{-1}=\sigma\phi$. The optical cross sections are independent of the photon flux, and, although they are not necessarily related to any particular microscopic absorption process, they facilitate the comparison of results from different measurements.

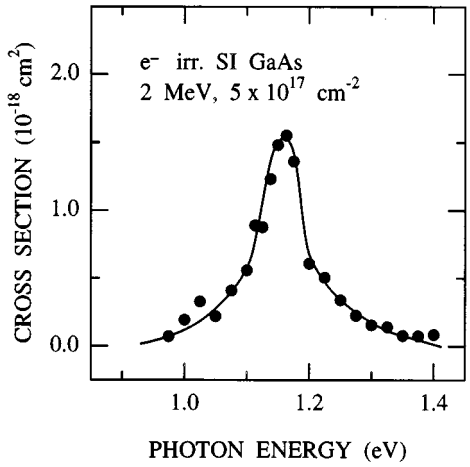

FIG. 5. Cross section for the decrease in infrared absorption under illumination in electron-irradiated GaAs as a function of the photon energy used for illumination. Measurement temperature was 25 K.

Results for the cross section σ_1, corresponding to the decrease in absorption, are presented in Fig. 5. The cross section is largest at a photon energy of 1.15 eV, and its value there is $\sigma_1(1.15\text{ eV})=1.6\times10^{-18}\text{ cm}^2$. Both the absolute value and the photon energy dependence of σ_1 agree well with the cross sections measured for the photoquenching of the native $EL2$ defect in as-grown GaAs; see, e.g., Refs. 17 and 31.

Absorption related to the native and irradiation-induced metastable defects can be distinguished by their different annealing properties. 1.075-eV illumination converts both defects to their metastable states. A subsequent annealing at 100 K recovers the irradiation-induced defect back to the stable state, whereas the native one remains in the metastable state. The photon-energy dependence of the absorption coefficient at this state of the samples is presented in Fig. 1 with a dotted line. The absorption coefficient is smaller than the initial absorption for all photon energies. The difference between the initial absorption spectrum (full line in Fig. 1) and that obtained after 1.075-eV photoquenching and 100-K annealing (dotted line) is plotted in Fig. 6 with filled circles. The shape of this spectrum is remarkably similar to that of the $EL2$ defect in as-grown GaAs.[30,32] The absolute values of the absorption coefficients are typical for native $EL2$ concentrations of the order of 10^{16} cm^{-3}.

The native metastable defects observed in both as-grown and electron-irradiated GaAs have similar absorption (Fig. 6) and photoquenching (Fig. 5) properties as the well-known native $EL2$ defect. The annealing stage of the metastable state at 120 K is also the same as that found for $EL2$. Therefore, the native metastable defect can be identified as the $EL2$ center. The native $EL2$ defect is thus also present in electron-irradiated GaAs, and it is metastable in the same way as in as-grown material.

The persistent increase in the absorption coefficient $\alpha(t)$ (Fig. 1) is proportional to the irradiation fluence Φ_{e^-} (Fig. 4), and it is thus related to a defect D created in electron

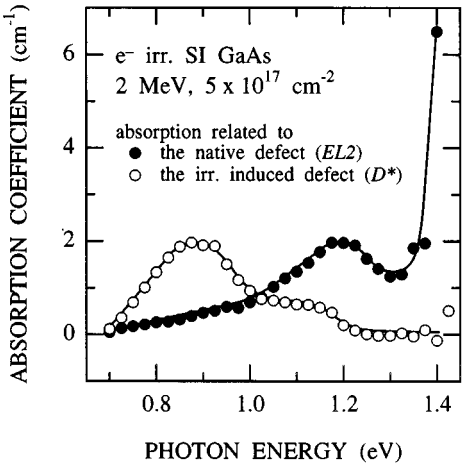

FIG. 6. Persistent changes in infrared absorption related to the native $EL2$ defect (solid circles) and to the metastable state D^* of the irradiation-induced defect (open circles) in electron-irradiated GaAs. Measurement temperature was 25 K.

irradiation. The increase in the absorption occurs with photon energies 0.95−1.15 eV, and it anneals out at 70 K. This defect thus has properties that are clearly different from those of the native $EL2$ defect.

After a sufficiently long illumination the absorption saturates to a value that is either smaller or larger than the initial absorption, depending on the illumination photon energy (see Fig. 2). To find out the photon-energy dependence of the absorption in this state of the sample where both native and irradiation-induced defects are in the metastable state, the IR absorption was measured after a 1.075-eV illumination that lasted for 25 000 s with a photon flux of 10^{16} cm^{-2} s^{-1}. The absorption spectrum in the 2-MeV electron-irradiated GaAs sample is plotted in Fig. 1 with a dashed line.

At photon energies 0.7 eV $<h\nu<$1.05 eV the absorption after 1.075-eV illumination is larger than the initial absorption, and for $h\nu>$1.05 eV it is smaller. For all photon energies this absorption is larger than or equal to the absorption measured after 100-K annealing. Since the metastable state of the native $EL2$ defect does not absorb light, the absorption after a long 1.075-eV illumination is due to the metastable state D^* of the irradiation-induced defect and to other defects present in the sample. Assuming that the absorption due to other defects is not affected by the illumination, the increased absorption related to the metastable state D^* is the difference between the spectra measured before and after the subsequent 100-K annealing, i.e., the difference between the dashed and dotted lines in Fig. 1. This difference is plotted in Fig. 6 with open circles. At photon energies 0.7 eV $<h\nu<$ 1.2 eV the metastable state D^* increases the total absorption, and at 0.9 eV the increase is largest.

IV. METASTABLE VACANCY AND IR ABSORPTION CONNECTED TO THE IRRADIATION-INDUCED DEFECT

A. Changes in IR absorption and appearance of the metastable vacancy

From the IR absorption results presented in the previous section, the following properties of the irradiation-induced defect D can be deduced: (i) it has a metastable state that is generated by 1.05−1.15-eV photons. (ii) The metastable state causes an increase in IR absorption, and (iii) it is annealed at 70 K. In earlier positron experiments electron irradiation has been found to produce metastable vacancies V^* in GaAs.[18] The aim of the present measurements is to find out whether the irradiation-induced metastable vacancy is related to the irradiation-induced defect D.

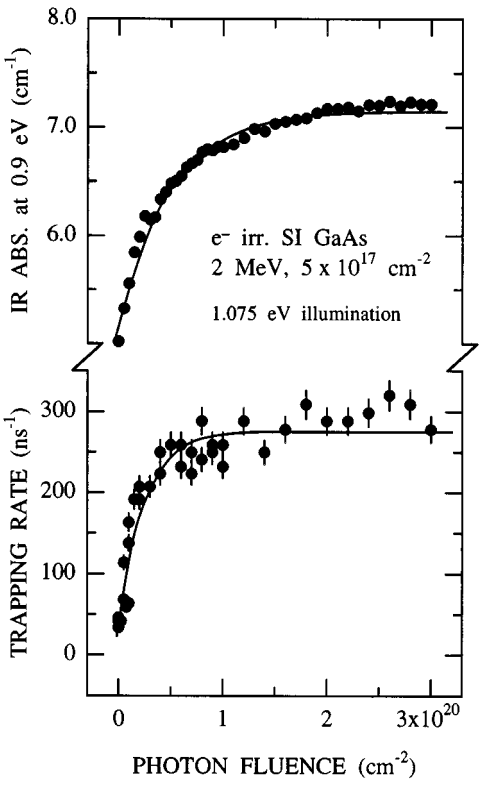

FIG. 7. Absorption at 0.9 eV and positron trapping rate at metastable vacancies as functions of 1.075-eV photon fluence in electron-irradiated GaAs. Measurement and illumination temperature was 25 K, and absorption and positron measurements were conducted between 1.075-eV illuminations.

The IR absorption and positron lifetime measurements were conducted at 25 K in the 2-MeV electron-irradiated sample aged at 300 K. Before the actual IR absorption and positron measurements the samples were illuminated with 1.075-eV photons with $\phi=10^{16}$ cm^{-2} s^{-1} for 3000 s whereupon annealing at 100 K took place. As explained in Sec. III D this procedure photoquenches the native $EL2$ defect but leaves the irradiation-induced defect D totally in the stable state. After the preliminary procedures, the sample was illuminated with 1.075-eV photons in sequence 20 times for 500 s and 10 times for 1000 s with a photon flux of 10^{16} cm^{-2} s^{-1}. Between these illuminations the absorption in the sample was monitored at 0.9 eV, where the most prominent changes related to the irradiation-induced defect take place (see Fig. 6 and Sec. III D).

The results are presented in the upper panel of Fig. 7 where the absorption at 0.9 eV is shown as a function of the 1.075-eV photon fluence ϕt. The absorption coefficient increases from 5.1 to 7.2 cm^{-1} during the generation process.

A single exponential function $\alpha(t) \propto \exp(-\sigma_{g,\alpha}\phi t)$ with a cross section $\sigma_{g,\alpha} = (2.0 \pm 0.5) \times 10^{-20}\ \mathrm{cm}^2$ can be fitted to the data.

Positron lifetime measurements were performed in darkness between similar 1.075-eV illuminations. The illumination caused the average positron lifetime to increase from the initial value of 234 ps and to saturate at 238 ps, indicating the generation of metastable vacancies. These metastable vacancies are either the irradiation-induced ones (V^*) or those related to the metastable state of the native $EL2$ defect ($EL2^*$), which also contains a vacancy.[17]

From the lifetime results it is possible to calculate the positron trapping rate at V^* and $EL2^*$, $\kappa(V^*) + \kappa(EL2^*)$, using Eq. (6). In addition to these metastable defects, positrons in electron-irradiated GaAs are trapped at irradiation-induced Ga vacancies ($\tau_v = 260$ ps) (Ref. 26) and Ga antisites ($\tau_{\mathrm{st}} = \tau_b = 230$ ps).[24] The positron trapping rates at these defects can be calculated from the temperature dependence of the average positron lifetime in darkness,[18,26] and the results are $\kappa(V_{\mathrm{Ga}}) = 45 \pm 5\ \mathrm{ns}^{-1}$ and $\kappa(\mathrm{Ga}_{\mathrm{As}}) = 330 \pm 50\ \mathrm{ns}^{-1}$ at 25 K. Trapping at Ga vacancies and Ga antisites is assumed not to change due to illumination, and for positron lifetime at the metastable vacancies $\tau(EL2^*) = \tau(V^*) = 245$ ps is used.[17,18]

The positron trapping rate at the metastable vacancies, $\kappa(V^*) + \kappa(EL2^*)$, is presented in the lower panel of Fig. 7 as a function of the 1.075-eV illumination fluence. The error estimation of κ takes into account only statistical errors in the average positron lifetime. At $\phi t = 0$ in Fig. 7, the positron trapping rate is 30 ns^{-1}. This value indicates the amount of positron trapping at the vacancy in the metastable state of the native $EL2$ defect [$\kappa(V^*) = 0$]. Taking $\mu(EL2^*) = 3 \times 10^{16}\ \mathrm{s}^{-1}$ (Ref. 33) an $EL2$ concentration of $[EL2] = \kappa(EL2^*)N/\mu(EL2^*) = 4 \times 10^{16}\ \mathrm{cm}^{-3}$ can be estimated from the positron data with Eq. (5). This concentration is in good agreement with the IR absorption results (Fig. 6 and Sec. III D).

With increasing illumination fluence, the trapping rate increases from 30 to 270 ns^{-1}, which is due to the generation of irradiation-induced metastable vacancies. As seen clearly in Fig. 7, the positron trapping rate increases almost simultaneously with the 0.9-eV absorption. The trapping rate can be modeled as $\kappa(t) \propto \exp(-\sigma_{g,\tau}\phi t)$, yielding the cross section $\sigma_{g,\tau} = (4.0 \pm 0.3) \times 10^{-20}\ \mathrm{cm}^2$ for the generation of metastable vacancies with 1.075-eV photons. Within a factor of 2 this cross section is the same as that determined above from the absorption experiments.

The dynamics of the optical recovery of the metastable defects was studied at 25 K with the following experimental procedure. A preparatory 1.075-eV illumination using a photon flux of $10^{16}\ \mathrm{cm}^{-2}\ \mathrm{s}^{-1}$ and lasting for 30 000 s was first used to generate the persistent increase in the IR absorption and the metastable vacancies to the sample. After this generation the sample was exposed to subsequent illuminations with 1.35-eV photons since an optical recovery has been earlier observed at this energy.[19] Between these illuminations the 0.9-eV absorption or the average positron lifetime was measured. The positron trapping rate at the metastable vacancies was calculated from the average lifetime as described above.

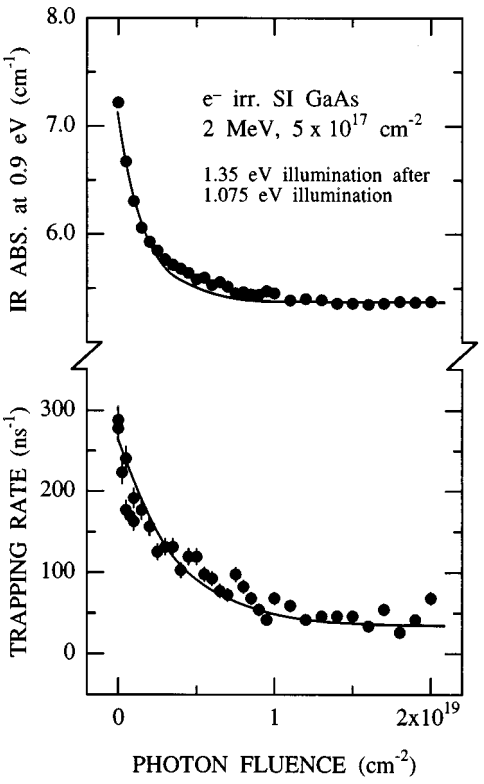

FIG. 8. Absorption at 0.9 eV and positron trapping rate at metastable vacancies as functions of 1.35-eV photon fluence in electron-irradiated GaAs. Illumination with 1.075-eV photons preceded 1.35-eV illuminations. Measurement and illumination temperature was 25 K, and absorption and positron measurements were conducted between 1.35-eV illuminations.

Figure 8 shows both the 0.9-eV absorption and the positron trapping rate at the metastable vacancy as functions of the 1.35-eV photon fluence. The absorption coefficient decreases from 7.2 to 5.3 cm^{-1} with the time constant corresponding to a cross section of $(5.5 \pm 0.5) \times 10^{-19}\ \mathrm{cm}^2$. Similarly, the positron trapping rate decreases from 270 to 30 ns^{-1} with a cross section of $(2.3 \pm 0.5) \times 10^{-19}\ \mathrm{cm}^2$. Here the trapping rate 30 ns^{-1} is again due to positron trapping at $EL2^*$, which thus does not exhibit any photorecovery.

The results of the IR absorption and positron annihilation measurements indicate that the metastable irradiation-induced vacancies are optically generated and recovered simultaneously with the persistent changes in the IR absorption. The simple exponential modeling of the IR absorption or positron data yields effective generation and recovery cross sections that are the same within a factor of 2. The increase in the absorption and generation of the metastable vacancies is therefore concluded to result from the same optical process.

It is worthwhile noting that the cross-section values presented here may not be purely related to the actual optical generation and recovery processes because both transitions may occur simultaneously. If the generation and recovery of the metastable state of defect D are modeled simply by

$$\frac{d[D]}{dt} = -\sigma_{\mathrm{gen}}\phi[D] + \sigma_{\mathrm{rec}}\phi[D^*],$$

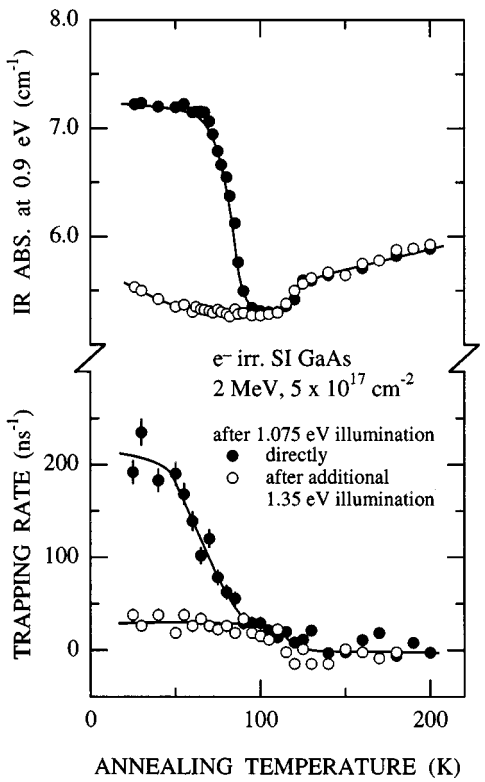

FIG. 9. Absorption at 0.9 eV and positron trapping rate at metastable vacancies as functions of annealing temperature in electron-irradiated GaAs. Isochronal annealing after 1.075-eV illumination is presented with solid circles and after additional 1.35-eV illumination with open circles. Measurement temperature was 25 K.

$$\frac{d[D^*]}{dt} = \sigma_{\text{gen}}\phi[D] - \sigma_{\text{rec}}\phi[D^*],$$

the time dependence of the solutions for $[D]$ and $[D^*]$ is $\exp[-(\sigma_{\text{gen}}+\sigma_{\text{rec}})\phi t]$. Rigorously, the experimentally observed cross section, e.g., $\sigma_{g,\tau}$ or $\sigma_{r,\alpha}$, is thus the sum of cross sections σ_{gen} and σ_{rec} related to the generation and recovery processes, respectively.

B. Annealing behavior of the IR absorption and the metastable vacancy

The isochronal annealing of the metastable vacancy can be quantitatively correlated with the 0.9-eV absorption in the experiments shown in Fig. 9. The sample was first illuminated for 30 000 s with 1.075-eV photons of a flux of 10^{16} cm^{-2} s^{-1}. After this, heat treatments were performed as described in Sec. III C, and absorption at 0.9 eV was monitored at 25 K between the treatments. As seen in Fig. 9, the absorption coefficient remains constant at 7.2 cm^{-1} until annealing at 65 K. At 65–90 K the absorption decreases to 5.3 cm^{-1}, whereupon it is constant until annealing at 120 K. After annealing at 120 K and higher temperatures the absorption increases gradually to 5.8 cm^{-1}, which is the initial value of the 0.9-eV absorption before any illumination and annealing treatments.

The average positron lifetime was measured as a function of the annealing temperature after 1.075-eV illumination lasting for 30 000 s. Lifetime τ_{av} remains at level 238 ps until annealing at 60–90 K gradually decreases the lifetime to a value of 235 ps. At 120 K a further decrease of about 1 ps occurs. Figure 9 shows with filled circles the positron trapping rate at the metastable vacancies, $\kappa(V^*)+\kappa(EL2^*)$, calculated from these lifetime results. The trapping rate behaves in the same way as the positron lifetime: it decreases during annealing at 60–85 K from 210 to 30 ns^{-1} and after annealing at 120 K to zero. The trapping rate of 30 ns^{-1} is due to the native $EL2$ defect (see Sec. IV A). The irradiation-induced metastable vacancy thus anneals at 70 K and the metastable vacancy related to $EL2^*$ at 120 K.

To check that the decrease in absorption after 1.35-eV illumination is indeed due to the same defect as the increased absorption after 1.075-eV illumination, a thermal annealing study was performed after 1.35-eV illuminations. In other words, the annealing study was conducted after similar illumination treatments as presented in Fig. 8. The results from the absorption and positron measurements are shown in Fig. 9 with open circles.

1.35-eV illuminations at 25 K decrease the 0.9-eV absorption from 7.2 to 5.5 cm^{-1} and the positron trapping rate from 210 to 30 ns^{-1}. As explained in Sec. IV A, this behavior is due to the photorecovery of the absorption coefficient and of the metastable vacancies. After the additional 1.35-eV illumination no annealing stages are observed in the 0.9-eV absorption at 70 K. However, at 120 K the absorption increases rapidly to 5.8 cm^{-1}. This stage is similar as that observed directly after the 1.075-eV illumination (Fig. 9). This indicates that the 1.35-eV illumination removes the persistent increase in absorption, but does not affect the metastability of the $EL2$ defect.

After additional 1.35-eV illumination, the average positron lifetime stays almost constant at 235 ps, until after annealing at 120 K it decreases to 234 ps. This lifetime change corresponds to the decrease in the trapping rate from 30 ns^{-1} to zero (Fig. 9). Hence, the 1.35-eV illumination recovers the irradiation-induced metastable vacancies but not the metastable vacancies connected to $EL2^*$.

The IR absorption data on the metastable defects in electron-irradiated GaAs can thus be perfectly correlated with the changes in the positron trapping rate. The positron results demonstrate the vacancy nature of the metastable state of the native $EL2$ defect in the electron-irradiated material. Furthermore, the metastable state of the irradiation-induced defect D can be associated with an increase in the positron trapping rate, indicating that this defect also has a vacancy in its metastable state.

V. NATURE OF THE IRRADIATION-INDUCED METASTABLE DEFECT

The observations in Sec. IV indicate that the defect that is responsible for the persistent increase in IR absorption in electron-irradiated GaAs has a vacancy in the atomic configuration of its metastable state. This vacancy is similar to that detected in the metastable state of the native $EL2$ defect, which is related to the arsenic antisite. The vacancy belonging to the metastable state of an arsenic antisite is in agreement with the vacancy-interstitial model for the metastability of an isolated arsenic antisite.[1] According to this model, the

arsenic antisite atom moves in the metastable configuration away from the lattice site in the [111] direction towards an interstitial position. Positrons detect the open volume associated with the metastable configuration, $As_{Ga} \rightarrow V_{Ga} - As_i$. Since a vacancy is observed in the metastable state of both the native $EL2$ and the irradiation-induced defect D, both these defects are related to the same defect, i.e., to the arsenic antisite.

However, some properties of the irradiation-induced As_{Ga} are clearly different from those of the native $EL2$ defect. The increased IR absorption and the optical recovery at low temperatures are not observed for the native $EL2$ defect or theoretically predicted for the isolated As antisite. This difference can be understood if the irradiation-induced As_{Ga} is not isolated but part of a defect complex.

In fact, a recent study with MCDA revealed an arsenic-antisite-related metastable defect in semi-insulating GaAs after electron irradiation.[16] The defect was identified as an arsenic-antisite–gallium-antisite pair[34] in which the metastability is associated with the lattice relaxation of As_{Ga}. The metastable state of this defect is optically generated with 1.05-eV photons and recovered with 0.8- or 1.35-eV photons. These properties are exactly the same as found for the irradiation-induced metastable vacancy and for the persistent increase in IR absorption in this work or earlier.[19] This similarity indicates that the metastable vacancy belongs to the atomic structure of the metastable irradiation-induced As_{Ga} complex observed in the MCDA experiments. However, the annealing stage of the metastable state of the As_{Ga} complex determined in this work (70 K) seems to differ from that reported in MCDA experiments (140 K according to Ref. 35).

According to the MCDA studies,[16,34] the As_{Ga}-Ga_{As} antistructure pair is not produced as a primary defect in electron irradiation, but rather formed in the annealing of primary defects at 200–300 K.[35] This statement is in agreement with the estimates of the introduction rates of defects in positron experiments. In 1.5-MeV electron irradiation the introduction rate of the defects containing the metastable vacancy is only 0.3 cm^{-1}, whereas one order of magnitude larger introduction rates have been determined for primary defects like V_{Ga} or Ga_{As}.[18,36] The low introduction rate suggests again that the irradiation-induced metastable defect is a complex rather than an isolated As_{Ga}.

The metastable state of the irradiation-induced As_{Ga} complex is responsible for the increased IR absorption. The magnitudes of the IR absorption caused by the generation and recovery processes of the metastable state can be estimated as follows. The positron trapping rate at the metastable vacancy V^* in the 2-MeV electron-irradiated sample is $\kappa(V^*) = 250\ ns^{-1}$ at 25 K. Taking the positron trapping coefficient $\mu(EL2^*) = 3 \times 10^{16}\ s^{-1}$ at 25 K,[33] concentration of the metastable vacancies is $[V^*] = \kappa(V^*)N/\mu(EL2^*) \approx 4 \times 10^{17}\ cm^{-3}$ [Eq. (5)]. The generation and recovery processes thus cause a change of $\Delta\alpha = \sigma[V^*] = 2 \times 10^{-20}\ cm^2 \times 4 \times 10^{17}\ cm^{-3} \approx 0.01\ cm^{-1}$ for 1.075-eV photons. However, the experimentally observed increase in absorption at this photon energy is about 0.7 cm^{-1} (Fig. 6), indicating that only about 1% of the absorption can be explained by the optical generation and recovery of the metastable state. The metastable state of the arsenic antisite complex is thus *itself* able to absorb IR light by optically exchanging electrons with the valence or conduction bands. The cross section for these photoionization processes can be roughly estimated as $\sigma = \Delta\alpha/[V^*] = 0.7\ cm^{-1}/4 \times 10^{17}\ cm^{-3} \approx 2 \times 10^{-18}\ cm^2$.

The fact that the metastable state of the irradiation-induced arsenic antisite complex is able to absorb light indicates that is has an ionization level in the energy gap. This is quite different from the experimental properties of the native $EL2$ defect. In the calculations performed for the isolated As_{Ga}, the $(-/0)$ ionization level of the metastable state is also slightly above the conduction-band minimum, i.e., not in the band gap.[1] However, very recent calculations for the arsenic-antisite–gallium-antisite pair show that the presence of the Ga antisite at the next-nearest-neighbor position of the As antisite atom modifies the electronic properties of the metastable state and causes ionization levels to appear in the energy gap.[37] Those ionization levels can explain the absorption properties of the metastable state of the As_{Ga} complex that were detected in this work.

The generation of the metastable state of the irradiation-induced As_{Ga} complex is most efficient at a photon energy of 1.05 eV, whereas for the native $EL2$ defect this energy is 0.1 eV larger. Furthermore, the optical cross section for the generation is also about 2 orders of magnitude larger for the native $EL2$ defect. According to the vacancy-interstitial model, the transformation of the isolated As_{Ga} defect to the metastable configuration occurs via an internal optical transition through an excited state of the defect.[1] The stable and the metastable states are separated by an energy barrier, and the transformation probability to the metastable state depends on the energy of the excited state and on the height of the barrier. The experimentally observed 0.1-eV shift downwards in the transition energy may indicate that the energy of the excited state of the As_{Ga} complex is below that of the $EL2$ defect when compared to the top of the energy barrier. This can dramatically reduce the transition probability to the metastable state thus explaining the experimentally observed small optical cross section. The barrier height for the recovery of the metastable state of the As_{Ga} complex is also much lower than that of the native $EL2$: the annealing temperature of 70 K for the complex corresponds to a barrier height of 0.2 eV whereas for $EL2$ the barrier height is 0.34 eV.

A very interesting explanation for the optical recovery of the As_{Ga} complex has been recently given by Pöykkö, Puska, and Nieminen in Ref. 37. According to their calculations, the metastable state of the As_{Ga}-Ga_{As} complex can recover optically through two different excited states of the defect. In fact, experimentally the metastable As_{Ga} complex can be recovered with two photon energies, 0.85 and 1.35 eV.[16,19] According to theory, the cross section can be expected to be much larger for the 1.35-eV recovery, because the excited state related to this transition may much more efficiently help the defect to overcome the 0.2-eV barrier. In experiments the optical recovery with 1.35-eV photons is indeed more efficient than with 0.85-eV photons.[19] Furthermore, the optical cross section for the 1.35-eV photorecovery ($\sigma_r \approx 5 \times 10^{-19}\ cm^2$) is more than an order of magnitude larger than the optical generation cross section for 1.05-eV photons ($\sigma_g \approx 2 \times 10^{-20}\ cm^2$); see Sec. IV A. This difference can also be easily understood: the state generated by 1.35-eV light is above that excited with 1.05-eV light[37] thus enabling more efficient transition over the energy barrier.

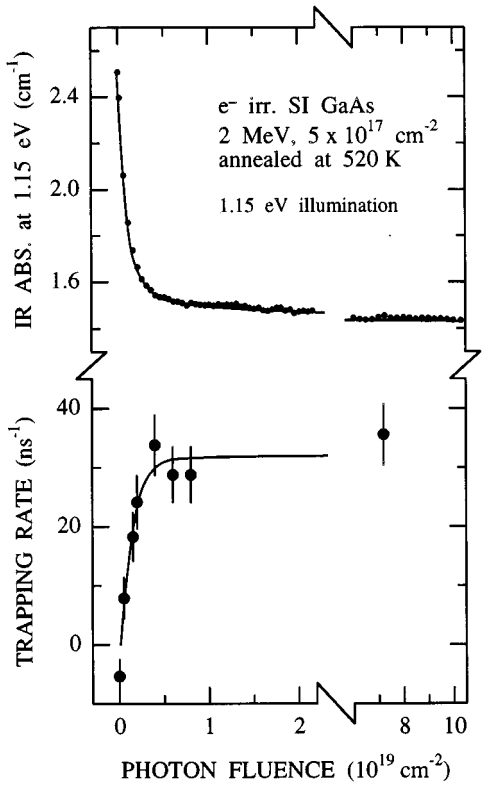

FIG. 10. Absorption at 1.15 eV and positron trapping rate at metastable vacancies as functions of 1.15-eV photon fluence in electron-irradiated GaAs annealed at 520 K. Measurement and illumination temperature was 25 K, and absorption and positron measurements were conducted between the 1.15-eV illuminations.

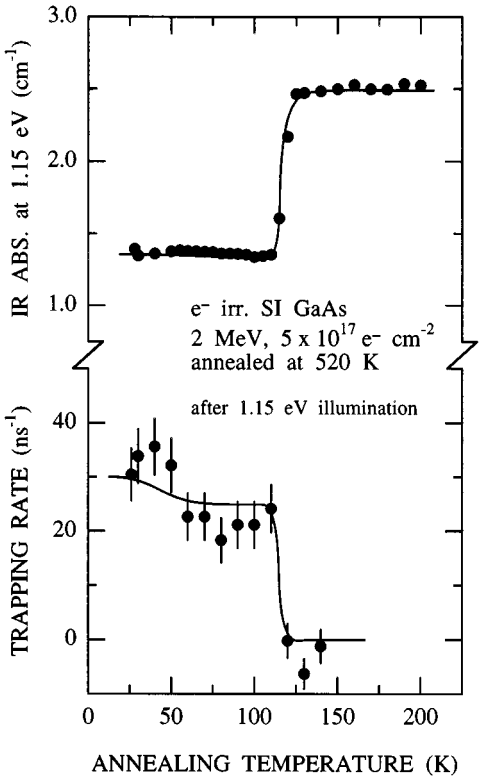

FIG. 11. Absorption at 1.15 eV and positron trapping rate at metastable vacancies as functions of annealing temperature in electron-irradiated GaAs annealed at 520 K. Illumination before annealing occurred with 1.15-eV photons. Measurement temperature was 25 K.

VI. THERMAL STABILITY OF THE IRRADIATION-INDUCED ARSENIC-ANTISITE COMPLEX

A. Experimental results on electron-irradiated GaAs after annealing at 520 K

One pair of the semi-insulating GaAs samples irradiated with 2-MeV electrons at 300 K was annealed at 520 K in order to study the thermal stability of the irradiation-induced As_{Ga} complex. After annealing at 520 K the IR absorption spectrum resembles closely that obtained in as-grown GaAs (Fig. 1). This indicates that most of the irradiation-induced defects have been annealed out. The disappearance of defects can also be observed in the positron results: the average positron lifetime was 233 ps at 25 K and only 234 ps at 300 K. These values are very near free positron lifetime in GaAs and much less than those measured after 300-K annealing. Positron trapping rates at the dominant defects V_{Ga} and Ga_{As} can be calculated similarly as in Sec. IV A or earlier,[18] and the results are $\kappa(V_{Ga})=13\pm6\ \mathrm{ns}^{-1}$ and $\kappa(Ga_{As})=110\pm60\ \mathrm{ns}^{-1}$ at 25 K. As these values are lower than those after 300-K annealing, these defects have mostly annealed at 520 K. This is in agreement with earlier positron results.[18,36]

The photoquenching of absorption at 25 K is presented in Fig. 10 for 1.15-eV illumination. The absorption coefficient $\alpha(t)$ decreases roughly exponentially from 2.5 to 1.4 cm^{-1}, and the changes in α are persistent. Hence, about 50% of the absorption can be photoquenched in the sample annealed at 520 K. The absorption curve in Fig. 10 yields an optical cross section of $(9\pm1)\times10^{-19}\ \mathrm{cm}^2$ for the photoquenching process. The decrease in absorption can be induced with 0.9−1.3-eV photons, and no increase in absorption is detected at any photon energy.

The generation of the metastable vacancies was studied by performing positron lifetime measurements in darkness at 25 K between 1.15-eV illuminations. As a function of 1.15-eV photon fluence the average positron lifetime increased from 233 to 236 ps. The increase in the average lifetime indicates the generation of metastable vacancies in the sample annealed at 520 K. The positron trapping rate at the metastable vacancies was calculated similarly as in Sec. IV A by assuming that the illumination does not affect the positron trapping at the Ga vacancies and Ga antisites present in the sample. The trapping rate at the metastable vacancy is presented in Fig. 10. The illumination time required for the positron trapping rate to saturate is a factor of 20 shorter than in electron-irradiated GaAs aged at room temperature. An exponential fit to the trapping rate versus illumination fluence yields an optical cross section of $(8\pm2)\times10^{-19}\ \mathrm{cm}^2$ for the generation of the metastable vacancies.

The annealing behavior of the persistent decrease in absorption as well as that of the metastable vacancy are presented in Fig. 11. The absorption coefficient after 1.15-eV illumination is 1.4 cm^{-1} and increases back to the initial value 2.5 cm^{-1} after annealing at 120 K. In positron results the same phenomenon is observed: after annealing at 120 K

the average lifetime decreases from 236 to 232 ps abruptly. As shown in Fig. 11, the corresponding decrease in the positron trapping rate at the metastable vacancy is from 30 ns^{-1} to zero.

B. Effects of 520 K annealing on electron-irradiated GaAs

In electron-irradiated GaAs annealed at 520 K the IR absorption and positron results differ from those obtained in irradiated GaAs aged at room temperature: no metastable increase in absorption connected to irradiation-induced As_{Ga} complexes is observed in the annealed material. The decrease in absorption under 1.15-eV illumination occurs with almost the same time constant as the generation of the metastable vacancy (Fig. 11). The optical cross section corresponding to this process is close to that for the photoquenching of the native $EL2$ defect in as-grown GaAs. After the photoquenching the changes in IR absorption and positron trapping rate recover in a single state at 120 K, and no effects are seen at 70 K. The absolute values of positron trapping rate at metastable vacancies correspond to the native $EL2$ concentration of the material, and the value 30 ns^{-1} (Figs. 10 and 11) is also the same as that determined in the 2-MeV electron-irradiated sample after annealing at 300 K (Sec. IV). The absolute accuracy of this value, however, is $30-50$ % and only the statistical errors are shown in Figs. 10 and 11.

The photoquenching and thermal-annealing properties of the metastable defects in the sample annealed at 520 K are exactly the same as those of the native $EL2$ defect. Therefore we conclude that the native $EL2$ is the only metastable defect present in the annealed material. The absence of the persistent increase in absorption and of the 70-K annealing stage indicate that the irradiation-induced As_{Ga} complex is not detected after the sample has been annealed at 520 K. However, the results of Sec. III C show that after annealing at 425 K this defect is still present. The thermal annealing of the irradiation-induced As_{Ga} complex thus occurs between 450 and 520 K.

The irradiation-induced defects in GaAs anneal in three main stages at 235, 280, and 520 K according to electrical, optical, electron-paramagnetic-resonance, and positron experiments.[18,26,36,38–40] In positron experiments these stages have been associated with Ga vacancies (200–300 K) and Ga antisites and As vacancies (500–600 K).[26,36,38] The results of this work suggest that, in addition to Ga antisites, As_{Ga} complexes anneal at around 500 K.

VII. CONCLUSIONS

The optical properties and atomic structure of metastable defects in electron-irradiated GaAs have been studied by infrared absorption and positron lifetime measurements. Systematic photoquenching and thermal annealing experiments allowed us to associate changes detected in the infrared absorption to the metastable defects observed by positron annihilation technique. Furthermore, measurements as a function of electron-irradiation fluence enabled the distinction between the native metastable defects and those induced by the irradiation.

Two different metastable defects can be observed in semi-insulating GaAs after electron irradiation and annealing at 300 K. The first one is present already in the as-grown material, and its concentration is not increased by the irradiation. The metastable state of this defect can be generated with $h\nu = 1.0-1.3$ eV photons, and the transition takes place most efficiently at $h\nu = 1.15$ eV with an optical cross section of 1×10^{-18} cm^2. The metastable state anneals thermally at 120 K, but it cannot be optically recovered at 25 K. No absorption related to the metastable state can be detected. These properties are identical to those of the native $EL2$ defect. Therefore, the $EL2$ defect is present after electron irradiation and exhibits similar metastable properties as in as-grown GaAs.

The second metastable defect is found only in irradiated material, and its concentration increases with the irradiation fluence. The defect is found after electron irradiation at 300 K, but it disappears after annealing at 520 K. Its metastable state can be generated with $h\nu = 0.95-1.2$ eV photons. The generation process is much less efficient than the photoquenching of the native $EL2$ defect, and the maximum cross section for the transition is only 2×10^{-20} cm^2 at $h\nu = 1.075$ eV. The metastable state can be optically recovered with $h\nu = 1.35$ eV photons with an optical cross section of 5×10^{-19} cm^2. The thermal annealing of the metastable state takes place at 70 K. The metastable state absorbs infrared light at $h\nu = 0.7-1.2$ eV in a photoionization process, indicating that it has ionization levels in the band gap.

The positron lifetime experiments show that both the native and irradiation-induced metastable defects have a similar vacancy in the structure of their metastable states. This vacancy can be associated with the metastable state of the As antisite defect, which is formed by a relaxation of the As atom towards the interstitial position.[1] However, the properties of the irradiation-induced metastable defect differ from those of the native $EL2$ defect or those found for the isolated As antisite in theoretical calculations. Therefore, the observed defect is attributed to a complex involving the As antisite. According to recent calculations,[37] the antistructure pair As_{Ga}-Ga_{As} detected earlier in MCDA experiments[16,34] has similar optical properties to those observed for the irradiation-induced As antisite complex in this work.

ACKNOWLEDGMENTS

We would like to thank Professor J.-M. Spaeth and Dr. K. Krambrock for the 2-MeV electron-irradiated GaAs samples. We have also benefited from many useful discussions with S. Pöykkö, Dr. M. J. Puska, and Professor R. M. Nieminen.

*Permanent address: INSTN, CE-Saclay, 91191 Gif-Sur-Yvette Cédex, France.

[1] J. Dabrowski and M. Scheffler, Phys. Rev. Lett. **60**, 2183 (1988); Phys. Rev. B **40**, 10 391 (1989); D. J. Chadi and K. J. Chang, Phys. Rev. Lett. **60**, 2187 (1988).

[2] A. Pillukat and P. Ehrhart, Appl. Phys. Lett. **60**, 2794 (1992).

[3] A. Pillukat and P. Ehrhart, Phys. Rev. B **45**, 8815 (1992).

[4] K. Krambrock, J.-M. Spaeth, C. Delerue, G. Allan, and M. Lan-

noo, Phys. Rev. B **45**, 1481 (1992).
[5] E. Christoffel, A. Goltzene, and C. Schwab, J. Appl. Phys. **66**, 5648 (1989).
[6] M. O. Manasreh and D. W Fischer, Phys. Rev. B **39**, 3871 (1989).
[7] M. O. Manasreh and D. W. Fischer, Appl. Phys. Lett. **53**, 2429 (1988).
[8] N. K. Goswami, R. C. Newman, and J. E. Whitehouse, Solid State Commun. **40**, 473 (1981).
[9] R. B. Beall, R. C. Newman, J. E. Whitehouse, and J. Woodhead, J. Phys. C **17**, 2653 (1984).
[10] H. J. von Bardeleben and J. C. Bourgoin, J. Appl. Phys. **58**, 1041 (1985).
[11] H. J. von Bardeleben, D. Stiévenard, D. Deresmes, A. Huber, and J. C. Bourgoin, Phys. Rev. B **34**, 7192 (1986).
[12] D. Stiévenard and J. C. Bourgoin, J. Appl. Phys **59**, 743 (1986).
[13] D. Stiévenard, X. Boddaert, J. C. Bourgoin, and H. J. von Bardeleben, Phys. Rev. B **41**, 5271 (1990).
[14] J.-M. Spaeth, K. Krambrock, and M. Hesse, Mater. Sci. Forum **143–147**, 217 (1994).
[15] A. Pillukat and P. Ehrhart, Mater. Sci. Forum **83–87**, 947 (1992).
[16] M. Hesse, F. K. Koschnick, K. Krambrock, and J.-M. Spaeth, Solid State Commun. **92,** 207 (1994).
[17] K. Saarinen, S. Kuisma, P. Hautojärvi, C. Corbel, and C. LeBerre, Phys. Rev. B **49**, 8005 (1994).
[18] K. Saarinen, S. Kuisma, J. Mäkinen, P. Hautojärvi, M. Törnqvist, and C. Corbel, Phys. Rev. B **51**, 14 152 (1995).
[19] S. Kuisma, K. Saarinen, P. Hautojärvi, and C. Corbel, Phys. Rev. B **53**, R7588 (1996).
[20] *Positrons in Solids*, edited by P. Hautojärvi, Topics in Current Physics Vol. 12 (Springer-Verlag, Heidelberg, 1979); *Positron Solid State Physics*, edited by W. Brandt and A. Dupasquier (North-Holland, Amsterdam, 1983).
[21] S. Kuisma, K. Saarinen, P. Hautojärvi, C. Corbel, and C. LeBerre, Phys. Rev. B **53**, 9814 (1996).
[22] M. J. Puska, C. Corbel, and R. M. Nieminen, Phys. Rev. B **41**, 9980 (1990).
[23] M. Manninen and R. M. Nieminen, Appl. Phys. A **26**, 93 (1981).
[24] K. Saarinen, P. Hautojärvi, A. Vehanen, R. Krause, and G. Dlubek, Phys. Rev. B **39**, 5287 (1989).
[25] J. Mäkinen, C. Corbel, P. Hautojärvi, P. Moser, and F. Pierre, Phys. Rev. B **39**, 10 162 (1989).
[26] C. Corbel, F. Pierre, K. Saarinen, P. Hautojärvi, and P. Moser, Phys. Rev. B **45**, 3386 (1992).
[27] J. Mäkinen, P. Hautojärvi and C. Corbel, J. Phys. Condens. Matter **4**, 5137 (1992).
[28] C. LeBerre, C. Corbel, K. Saarinen, S. Kuisma, P. Hautojärvi, and R. Fornari, Phys. Rev. B **52**, 8112 (1995).
[29] R. N. West, in *Positrons in Solids*, edited by P. Hautojärvi, Topics in Current Physics Vol. 12 (Springer-Verlag, Heidelberg, 1979), p. 89.
[30] M. Kaminska and E. R. Weber, in *Imperfections in III/V Materials*, Semiconductors and Semimetals Vol. 38, edited by E. R. Weber (Academic Press, New York, 1993).
[31] G. Vincent, D. Bois, and A. Chantre, J. Appl. Phys. **53**, 3643 (1982); E. Christoffel, A. Goltzene, and C. Schwab, J. Appl. Phys. **66**, 5648 (1988); M. O. Manasreh and D. W. Fischer, Phys. Rev. B **40**, 11 756 (1989).
[32] G. M. Martin, Appl. Phys. Lett. **39**, 747 (1981).
[33] C. LeBerre, C. Corbel, M. R. Brozel, S. Kuisma, K. Saarinen, and P. Hautojärvi, J. Phys. Condens. Matter **6**, L759 (1994); S. Kuisma, K. Saarinen, P. Hautojärvi, Z.-Q. Fang, and D. Look, J. Appl. Phys. (to be published).
[34] K. Krambrock and J.-M. Spaeth, Phys. Rev. B **47**, 3987 (1993).
[35] F. K. Koschnick, M. Hesse, K. Krambrock, J. M. Spaeth, in *Semi-insulating III-V Materials*, edited by M. Godlewski (World Scientific, Singapore, 1994).
[36] K. Saarinen, A. P. Seitsonen, P. Hautojärvi, and C. Corbel, Phys. Rev. B **52**, 10 932 (1995).
[37] S. Pöykkö, M. J. Puska, and R. M. Nieminen, Phys. Rev. B **55**, 6914 (1997).
[38] C. Corbel, F. Pierre, P. Hautojärvi, K. Saarinen, and P. Moser, Phys. Rev. B **41**, 10 632 (1990).
[39] K. Thommen, Radiat. Eff. **2**, 201 (1970).
[40] Y. Q. Jia, H. J. von Bardeleben. D. Stiévenard, and C. Delerue, Mater. Sci. Forum **83–87**, 965 (1992).